Experimental Investigation about Capillary Properties of Braided Wire Wick for Heat Pipe

Yohan Kim, Hyungdae Kim*
Department of Nuclear Engineering, Kyung Hee University, Republic of Korea
Corresponding author: hdkims@khu.ac.kr

***Keywords : heat pipe, braided wire wick, capillary property, capillary rate-of-rise experiment**

1. Introduction

A heat pipe-cooled reactor is receiving attention as an energy source in remote areas such as space because of its advantages in simplicity and reliability with a passive cooling system. A heat pipe, which is the reliable passive cooling system of the heat pipe-cooled reactor, requires no moving parts like turbomachinery and has a high thermal conductivity. Thus, it has been used in a variety of space missions.

The Korea Atomic Energy Research Institute (KAERI) is developing a heat pipe-cooled reactor for lunar surface power. In the development, one of the key parts is the design of bendable heat pipes. The bendable heat pipe is essential for maximizing utilization in the space heat pipe reactor. For bendable heat pipes, it was reported from previous studies that conventional wicks such as grooved, sintered powder, and screen wicks are deformed by bending and cause irreparable damage or separation from a container wall [1, 2]. This kind of deformation can limit the heat transport capability of the heat pipes [1]. Thus, KAERI suggested a spring-like braided wire wick structure for the bendable heat pipes as it has reliable bending capability due to high elasticity [3].

In the design process of the heat pipe, its operating limits, which are heat transport limits such as capillary limit and entrainment limit, must be investigated. The capillary limit is affected by the capillary-driven flow characteristics in the wick, and they are affected by the capillary properties of the wick, which is a porous media. Especially, an effective capillary radius and permeability are the capillary properties of the wick and are one of the governing parameters of the capillary limit. Therefore, these kinds of braided wire wick capillary properties must be investigated to predict the operating limits of the bendable heat pipes.

However, the braided wire wick lacks research and no model was identified to predict the capillary properties unlikely with other conventional wicks, such as grooved, sintered powder, and screen wicks. The properties of wicks with complex geometries must be determined by experiments [4]. Therefore, the properties of the braided wire wick should be measured experimentally.

In this study, two capillary properties, the effective capillary radius and the permeability were measured and investigated experimentally. Furthermore, due to its elasticity, the braided wire wick is deformed when it is inserted in the heat pipe, so the effect of the deformation on the properties was investigated together. As an experimental method, a capillary rate-of-rise experiment [5] was chosen because, using this method, the effective capillary radius and the permeability can be measured by one experiment.

2. Theoretical analysis

In capillary rise phenomenon, the maximum capillary pressure, $\Delta P_{c,max}$ is balanced by viscous loss and hydrostatic pressure. The viscous pressure drop in the porous medium can be expressed using Darcy's law [5, 6] while the liquid inertia term can be neglected due to the low liquid velocity. The resulting expression of the liquid rise in the wick can be given as Eq. 1.

(1) $$\Delta P_{c,max} = \frac{2\sigma}{r_{eff}} = \frac{\mu\varepsilon}{K} h(t) \frac{dh(t)}{dt} + \rho g h(t)$$

where σ, μ, ρ are surface tension, viscosity, and density of liquid, respectively, g is the gravitational acceleration, and $h(t)$ is the liquid rise height with respect to time.

In Eq. (1) appear three characteristic properties of the wick structure, including r_{eff}, K, and ε. The first characteristic property of the wick is the effective capillary radius, r_{eff}, which indicates the maximum curvature of a liquid meniscus in the wick structure [4],

(2) $$\frac{2}{r_{eff}} = \left(\frac{1}{R_1} + \frac{1}{R_2}\right)_{max}$$

where R_1 and R_2 are the principal radii of curvature of the meniscus. Another characteristic property of the wick in Eq. (1), K, is the permeability as the intrinsic property of the porous medium based on Darcy's law [6]. The last characteristic property of the wick is the porosity, ε, which is defined as the ratio of the void volume and the wick's total volume.

Solving differential equation (1) for the rise height, we can get the liquid rise height as a function of time.

(3) $$h(t) = A[1 + W(-\exp(-1 - Bt))]$$

(4) $$A = \frac{2\sigma}{r_{eff}\rho g}$$

(5) $$B = \frac{K g^2 \rho^2 r_{eff}}{2\sigma\mu\varepsilon}$$

where the function $W(x)$ is a Lambert W-function [7]. By carrying out a non-linear curve fitting the entire experimental data set with the rise height function, we can obtain the values of coefficients in the rise height function, A and B in Eq. 4 and Eq. 5, respectively.

The effective capillary radius and permeability can be obtained from those coefficients using the properties of the liquid. Additionally, it is confirmed that the maximum capillary pressure is equal to the hydrostatic pressure at the steady state because, as time goes infinitely, the value of the Lambert W-function approaches zero.

3. Experiments

3.1. Preparation of Samples

The used samples were the same braided wire wick that KAERI suggested. Two kinds of braided wire wick samples were prepared for the experiments to investigate the effect of the insertion into the heat pipe. The first sample, named by “Bare”, was the bare braided wire wick, and the second, named by “Acrylic-tube-inserted”, was the braided wire wick inserted in the acrylic tube, which was a simulant of the heat pipe’s container, whose inner diameter was 12.8 mm. By comparing the capillary performances of the two samples, the effect of inserting in a tube was investigated. Each sample had a cylindrical geometry. Side and cross-sectional views of each sample are shown in Fig. 1 and Fig. 2.

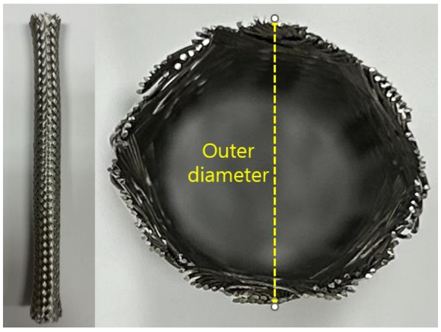

Fig. 1. Side and cross-sectional views of the bare braided wire wick sample.

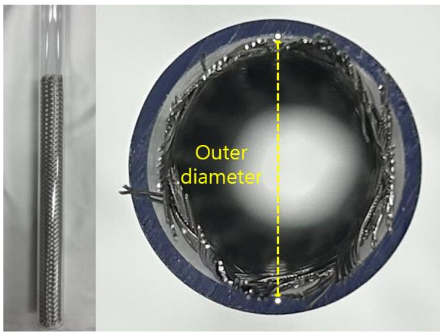

Fig. 2. Side and cross-sectional views of the acrylic-tube-inserted braided wire wick sample.

The main design parameters of the samples are summarized in Table I. The length, thickness, and outer diameter of each sample were measured using a vernier caliper and the uncertainty of these values is 0.1 mm. The porosity of the acrylic-tube-inserted sample is a calculated value defined as the ratio of the volume of the steel wires to the total volume of the wick [3]. The braided wire wick was shrunk radially and extended axially when it was inserted into the acrylic tube. To consider the effect of the deformation, the porosity of the bare sample was calculated, and it was slightly larger than the acrylic-tube-inserted sample.

Table I. Main design parameters of the samples.

Sample	Bare	Acrylic-tube-inserted
Wire diameter	0.2 mm	0.2 mm
Length	140.4 mm	144.0 mm
Wick thickness	1.1 mm	1.1 mm
Outer diameter	14 mm	12.8 mm
Porosity	0.818	0.805

Both samples were cleaned before experiments for 15 minutes using an ultrasonic cleaner with approximately 50°C of deconex 11 UNIVERSAL alkalic cleaning solution of company Borer Chemie AG. The acrylic tube and liquid reservoir were also cleaned for 10 minutes using an ultrasonic cleaner with deionized (DI) water. These cleaned apparatuses were dried in the air for 30 minutes at approximately 40°C.

3.2. Experimental setup and method

The liquid was 1atm, 17.2°C DI water. Each sample was inserted into the liquid reservoir about 2mm during the experiments and the rising time was measured since the wick contacted with the liquid. After the sample was inserted, the rising of the liquid was observed using a high-speed camera with the frame rate of 10 frames per second. In the pre-test of the experiment, it was observed that it needs over 300 seconds to detect the steady-state of the liquid rise and because the total frame number of the camera is limited, the smallest frame speed of the camera was chosen to set aside sufficient observing time of 800 seconds and detect the steady-state of the liquid rise.

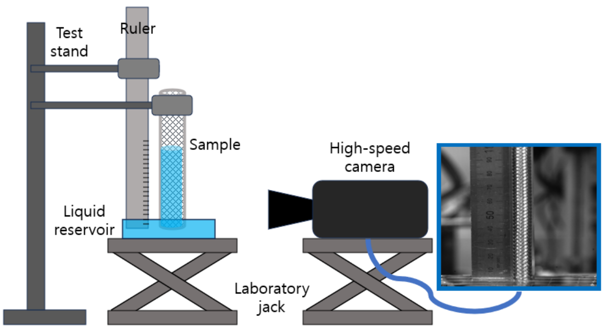

Fig. 3. The schematic of the capillary rate-of-rise experimental setup.

The schematic of the experimental setup is shown in Fig. 2. The rising height with respect to the time was measured from frame-by-frame analysis of the high-speed video using the open-source image analysis software, ImageJ. Variations of grey values of pixels by the liquid were observed due to its low reflectivity, and the heights were measured with the ruler whose minimum gradation was 0.5 mm. Then the data of measured heights were fitted with the function (3) using the commercial engineering software, MATLAB.

4. Results and Discussion

The movement of the liquid made the variations of the grey values in the images. A total of 8000 frames were investigated, and it was observed that in the area where the liquid moved, the grey values of the pixels were decreased, which had been darkened. The locations of the variations were compared with the ruler and the rise height of the liquid was measured. One of the observed variations and the schematic of the height measurement are shown in Fig. 4. The time steps between each frame in Fig. 4 are 0.4 seconds.

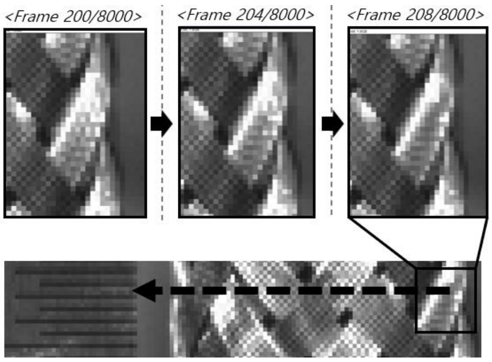

Fig. 4. The variations of the grey values in each frame and the schematic of the height measurement.

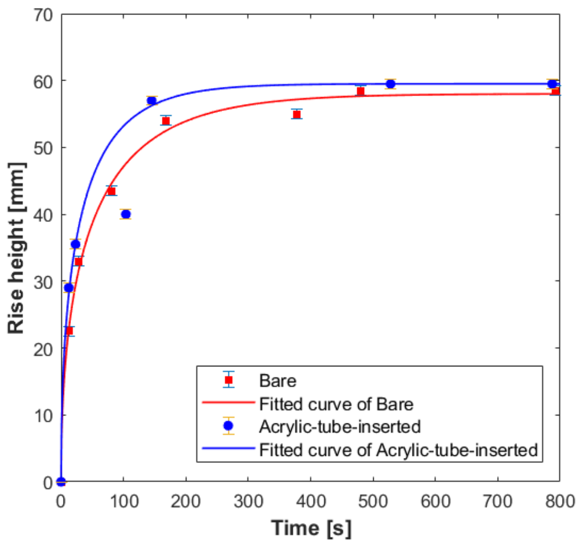

Fig. 5. Liquid rise height with respect to the time and fitted curves of the two samples: Bare (red) and Acrylic-tube-inserted (blue)

The liquid rise heights with respect to the time of both samples are shown in Fig. 5. The fitted curves are Eq. 6 and Eq. 7 for the bare and acrylic-tube-inserted samples, respectively.

$$(6) \quad h_B(t) = 58.0132[1 + W(-\exp(-1 - 0.0086t))]$$

$$(7) \quad h_A(t) = 59.5177[1 + W(-\exp(-1 - 0.0135t))]$$

The effect of the insertion into the acrylic tube was negligible since there was no significant difference between the capillary performances of the two samples.

Table II. Effective capillary radius and permeability of the braided wire wick samples.

Sample	Bare	Acrylic-tube-inserted
r_{eff} [mm]	0.257	0.251
K [mm^2]	4.5×10^{-5}	7.1×10^{-5}

The capillary properties were obtained by comparing coefficients of Eq. 4 and Eq. 5 with coefficients A and B of Eq. 3. The thermophysical properties of the water were obtained from the website of the National Institute of Standards and Technology (NIST). Measured values of the effective capillary radius and permeability are summarized in Table. II.

In the case of the effective capillary radius, both samples had values of approximately 0.2 mm, which was the wire diameter of the braided wire wick, and it was observed that the liquid mainly moved through the gap between the wires. Therefore, it can be thought that the wire diameter of 0.2 mm was working as a characteristic length scale of capillary flow in the braided wire wick.

On the other hand, a permeability calculated by a semi-empirical correlation for tightly wrapped wicks [8] can be considered as the theoretical prediction of the permeability, and the value is as follows.

$$(8) \quad K = \frac{d_{wire}^2 \varepsilon^3}{122(1-\varepsilon)^2} = 5 \times 10^{-3}\mathrm{mm}^2$$

where d_{wire} is the wire diameter. However, the prediction of Eq. (6) is approximately 100 times different from the measured values.

This kind of difference was observed in the analysis of a previous study about a braided wire wick. The same process as the present work was conducted for the experimental result of the previous study [9] to obtain permeability. The chosen experimental data from the study was for a sample that had no surface modification. The estimated function of rise height is Eq. 9.

$$(9) \quad h_R(t) = 44.4363[1 + W(-\exp(-1 - 0.0860t))]$$

The permeability was obtained using Eq. 9 and compared with the theoretical prediction by Eq. 8. The results of the analysis are summarized in Table III. The thermophysical properties of ethanol were obtained from a reference [10].

The obtained permeability was 3.73×10^{-1} mm^2, which was 3 orders of magnitude larger than the value in the previous analysis, which was 3.33×10^{-4}mm^2 [3]. The difference seems to appear because the method used to obtain the permeability in the present study utilized the whole data of the experiment while the method used in the previous analysis utilized a part of the experimental data within a narrow time interval. When a part of the experimental data in a relatively short time interval is utilized, the value of the obtained permeability could depend on the choice of the investigator. Thus, the present analysis method to fit a whole data set from a capillary rate-of-rise experiment might reduce uncertainty in measuring permeability.

Table III. Experimental condition of the previous study [9] and comparison of permeability.

Material of wick	Copper wire
Porosity of wick	0.736
Liquid	Ethanol
Temperature [K]	300
K (Experimental) [mm^2]	3.73×10^{-1}
K (Eq. 8) [mm^2]	1.17×10^{-4}

There was approximately 1000 times difference between the two values of permeability in Table III. It seems that these differences in permeability are due to the structural difference between the braided wire wick and the screen wick. Thus, further theoretical and experimental studies are needed to develop a correlation for permeability of braided wire wicks.

5. Conclusions

In this study, the capillary rate-of-rise experiment was conducted to investigate the capillary performance of the braided wire wick. The bare and acrylic-tube-inserted braided wire wick samples were tested.

By comparing the experimental results of the two samples, both showed similar capillary rise behaviors and capillary properties, so the effect of the insertion into the tube was negligible.

As the wick properties measurement, the effective capillary radius and permeability of the samples were measured. The wire diameter worked as a characteristic length scale for the capillary flow in the braided wire wick because both samples have the values scale of the wire diameter, 0.2 mm. On the other hand, the permeability showed a significant difference with the wrapped screen wick and thus a correlation for the permeability of the braided wire wick needs to be developed by additional experiments.

Acknowledgment

This work was supported by the National Research Council of Science & Technology (NST) grant funded by the Korea government (MSIT). (No. CAP23061-100)

REFERENCES

[1] Odhekar, D., & Harris, D. K., Experimental investigation of bendable heat pipes using sintered copper felt Wick., Thermal and Thermomechanical Proceedings 10th Intersociety Conference on Phenomena in Electronics Systems, 2006

[2] Beard, D. et al., Sodium heat pipes for space and surface fission power., 15th International Energy Conversion Engineering Conference, 2017

[3] Park, B. H. and Kim, C. S., Characteristic of Braided Wire Wick Heat Pipe for Heat Pipe Cooled Reactor, Transactions of the Korean Nuclear Society Virtual Spring Meeting July 9-10, 2020

[4] Chi, S. W., Heat Pipe Theory and Practice, New York: McGraw-Hill., 1976

[5] Elkholy, A., Durfee, J., Mooney, J. P., Robinson, A. J., and Kempers, R., A rate-of-rise facility for measuring properties of Wick Structures. Measurement Science and Technology, 34(4), 045301, 2023

[6] Neuman, S. P., Theoretical derivation of Darcy's law. Acta Mechanica, 25(3-4), 153-170, 1977

[7] Barry, D. A., Parlange, J.-Y., Li, L., Prommer, H., Cunningham, C. J., and Stagnitti, F., Analytical approximations for real values of the lambert w-function, Mathematics and Computers in Simulation, 53(1-2), 95-103, 2000

[8] B. Marcus, Theory and design of variable conductance heat pipes, NASA CR-2018, 1972

[9] Y. Tang et al., Experimental investigation of capillary force in a novel sintered copper mesh wick for ultra-thin heat pipes, Applied Thermal Engineering, Vo. 115, pp. 1020-1030, 2017

[10] Arnautovic, Z. et al., Measurements of thermophysical properties of ethanol + hexamethyldisiloxane and ethanol + octamethyltrisiloxane mixtures in the temperature range of 293-343 K at 100kPa., Journal of Chemical &ampl Engineering Data, 68(9), 2023